RSC Advances

ROYAL SOCIETY OF CHEMISTRY

www.rsc.org/advances

Hyperbranched polyol decorated carbon nanotube by click chemistry for functional polyurethane urea hybrid composites

Sasidhar Kantheti[a], Rohit Ranganathan Gaddam[a,b], Ramanuj Narayan[a], K.V.S.N Raju[a]*

[a] CSIR-Indian Institute of Chemical Technology, Hyderabad -500007, INDIA

[b] Amity Institute of Nanotechnology, Amity University, Noida-201301, INDIA

K. V. S. N. Raju,

Division of Polymers & Functional Materials, Indian Institute of Chemical Technology, Hyderabad-500007, India

E-mail: kvsnraju@iict.res.in; drkvsnraju@gmail.com

ABSTRACT

In the present work we report a facile decoration of multi-walled carbon nanotubes with hyperbranched polyether polyol using copper (I) catalyzed azide- alkyne click reaction in order to create hydroxy terminal groups. This decoration has been designed to improve the dispersibility of CNT in polymer matrix. These hydroxy functional decorated CNTs were then dispersed into poly (tetramethylene ether) glycol (PTMG) at different weight percentages to get the hybrid pre-polymers. These pre-polymers were reacted with 1-isocyanato- 4-[(4-isocyanatocyclohexyl) methyl] cyclohexane (H_{12}-MDI) at NCO/OH ratio of 1.2:1 and cured under atmospheric moisture to get the functional polyurethane -urea- CNT hybrid composites. There has been substantial improvement in the thermal stability, mechanical strength, corrosion resistance and antimicrobial activity of the polyurethane hybrid composites with the increase in carbon nanotube loading in pre-polymers. For example, with 2 wt% loading of carbon nanotubes, the tensile strength of the polyurethane hybrid composite improved from 1.25 N/mm^2 to 6.25 N/mm^2; water contact angle improved from 54° to 108° and also the rate of corrosion reduced from 0.047 mm/year to 0.0019 mm/year. We also observed that these hybrids possess remarkable shape recovery properties. These results demonstrate that the decorated CNT can be used as high performance additive for improving various properties of polyurethane hybrids in cost effective and eco-friendly ways.

1. Introduction

Carbon nanotubes (CNTs) are amongst the most researched allotrope of carbon since the past decade because of its high aspect ratio, unique structure, outstanding electronic, thermal, optical and mechanical properties.[1-4] Due to their excellent mechanical properties, very small amount of incorporation of CNTs into a polymer matrix could lead to hybrid composites having superior physico-chemical, mechanical, thermal, and bacterial resistance properties.[5-9] In general, incorporation of CNT into polymer matrices not only improves the overall physico- chemical properties of the composite but also inculcates additional properties like shape recovery, hydrophobic and anti-corrosive behaviors. Shape recovery polymers have an edge over their shape-memory alloy counterpart since they have adjustable transition temperature, highly stable shape, easy shaping, cost effective and easy processibility.[10-12] Shape memory polymer materials have wide range of applications as coating materials, elastomeric materials, medical applications, actuators, textiles and many more. Polyurethane based shape memory polymers is amongst the most researched one, owing to its hard and soft segments which are microphase separated heterogeneous structure. The soft segment of the polymer helps in fixation of the shape acting as a molecular switch whereas the hard segment which has an inherently high melting point enables effective cross-linking. In the view point of shape recovery materials, CNTs could fill the role of being very effective filler for enhancing high shape recovery and shape recovery force. This property is attributed again to the CNT's high thermal conductivity coefficient and excellent mechanical properties.

The improvement of composite properties depends directly on the dispersibility and interfacial interactions of CNT with polymer matrix.[13] The dispersion of pristine CNTs is very difficult due to their insolubility in both organic and inorganic solvents. Therefore, surface modifications are made in order to make CNTs processable and soluble.[14] The surface of Multi-walled carbon nanotubes (MWCNTs) and single-walled carbon nanotubes (SWCNTs) can be functionalized by both covalent[15-17] and non-covalent[18-21] means. A non-covalent functionalization involves surface modification of CNTs via π-π staking interactions, van der walls interaction, physical entanglement, electrostatic adsorption or hydrogen bonding without disturbing the extended π -conjugation of the nanotubes.[22] In contrast, a covalent functionalization requires formation of strong chemical bond between CNTs and the moieties to be attached. Oxidation of CNTs is the

most simple covalent modification which terminates the CNT surface with a carboxyl group (–COOH) or hydroxyl groups (–OH). The oxidation of CNT can be achieved by either direct exposure of CNTs to fixed air or oxygen, treatment with nitric acid, mixture of aqueous hydrogen peroxide and sulphuric acid, acid mixtures etc.[23] It is very pertinent to have –COOH group, because of its versatility in providing many different chemical reactions to occur on CNT surface.[24] Further the –COOH group could be modified with various molecules to obtain the necessary surface termination. The mechanical, thermal and optical properties depend on the π conjugations of CNT.

The covalent modification of CNTs with hyperbranched polymers (HBPs) is one of the promising ways to impart superior properties to CNTs. These branched polymers are macromolecules with three-dimensional architecture, which possess excellent solubility, low melt viscosity, broader molar mass distribution and extremely high density of functional groups at the surface.[25] A major advantage of HBPs is that, they possess large number of terminal functional groups which could be further exploited by coupling them with other materials like fluorophores, dyes and other electroactive groups.[26] Anchoring HBPs on CNTs could be achieved by a variety of well established reactions. Click chemistry has been used to attach liner polymers to CNTs, however, HBP attachment is still unexplored. Among all click reactions, copper(I) catalyzed azide-alkyne 1,3-dipolar cycloaddition reaction is most popular in polymer and material science because it provides high quantitative yield, high tolerance of functional groups[27], simple reaction conditions and insensitivity to solvents and reaction medium[28], high chemo selectivity with no side products, chemical inertness of 1,2,3-triazole ring and ease of the product isolation. Thus, employing click chemistry is a feasible approach for surface functionalization of CNTs with polymer.[29]

Hence in the present study we report a novel and easy approach for the modification of CNT with hyperbranched polymer using click chemistry for the preparation of functional polyurethane-urea- CNT hybrid composites. Initially the carboxyl terminated CNTs (CNT-COOH) were converted to alkyne terminated CNT (CNT-Alkyne) by esterification with propargyl alcohol. The obtained CNT-Alkyne was treated with an azide terminated hyperbranched polyol (HBP-N_3) by click reaction in order to obtain hydroxyl terminated and hyperbranched polyol decorated CNT (CNT-HBP). The various steps involved in surface

modification were confirmed by Thermo gravimetric analysis (TGA), Field emission Scanning electron microscopy (FE-SEM), Transmission electron microscopy (TEM),X-Ray diffraction (XRD), Fourier transform infrared (FT-IR) and Raman spectroscopic techniques. The obtained CNT-HBP was loaded in different weight percentages such as 0.5, 1 and 2 into poly (tetramethylene ether) glycol (PTMG) matrix. These pre-polymers were reacted with 1-isocyanato- 4-[(4-isocyanatocyclohexyl) methyl] cyclohexane (H_{12}-MDI) at NCO/OH ratio of 1.2:1 and cured under atmospheric moisture to get the functional polyurethane -urea- CNT hybrid composites. The resulting Polyurethane-urea-CNT hybrids along with pure polyurethane were analyzed by TGA, Universal testing machine (UTM), Atomic force microscopy (AFM), XRD, FT-IR, FE-SEM, water contact angle, antimicrobial and electrochemical polarization studies.

2. Experimental section

2.1. Materials

Pristine Multi Walled CNTs (purity 95%, 15-20 nm in diameter (PlasmaChem GmbH) were used without further purification. Trimethylolpropane (TMP), Propargyl alcohol, Boron tiflouride diethyl etherate, Copper (I) Iodide were purchased from Aldrich Chemicals (Milwaukee, WI, U.S.).Epichlorohydrin, acetonitrile, Sodium Azide, Chloroform, Anhydrous Triethylamine, Tetrahydrofuran (THF), Dimethyl Formamide, Tetra butyl ammonium bromide (TBAB), Diisopropyl ethylamine (DIPEA), Ammonia solution ($NH_3.H_2O$) were purchased from Finar Reagents, Mumbai, India.

2.2. Characterizations

Fourier transform IR spectra (FTIR) of synthesized samples recorded by Thermo Nicolet Nexus 670spectrometer.The ^{1}H and ^{13}C NMR of the synthesized samples were done inVARIENE-200 and BRUKER-300 MHz spectroscopy by taking tetra methyl silane (TMS) as standard at room temperature and dissolving in DMSO-d_6 solvent. Mass spectra (ESI-MS) of synthesized hyperbranched polyols were recorded on a LC-MSD-Trap-SL mass spectrometer. XRD patterns for the all the samples were obtained using a Siemens D-5000 X-ray diffractometer with Cu Kα radiation of wavelength 1.54. The thermo gravimetric analysis was conducted on TGA Q500 Universal TA instrument (U.K) at temperature ramp rate of 10^0C min^{-1} from 25 to 600°C with a

continuous N_2 flow at the rate of 30 ml min^{-1}.Raman spectra was recorded using Horiba JobinYvon Raman spectrometer with a laser excitation wavelength of 632.81nm. The changes in morphology of MWCNTs due to surface modification were observed under FESEM using S4300 SEIN HITACHI Japan at 10 kV. The samples were coated with a thin gold layer of ~5 nm of thickness by sputtering process to make them conducting for SEM analysis.

2.3. Synthesis of chlorinated hyperbranched polyether polyol (HBP-Cl)

The chlorinated hyperbranched polyol was prepared according to a previous report.[30] Trimethylolpropane (2gm, 14.9 mmol, 1eq) was taken into a single neck round bottom flask equipped with nitrogen inlet and a magnetic stirrer. Initially TMP was heated at 56°C up to melt. After complete melting the heat was removed and 0.01ml of BF_3 etherate was added as a catalyst. To this reaction mixture epichlorohydrin (4.13 gm, 44.7 mmol, 3eq) was added drop wise for a period of 10 minutes. After complete addition the reaction mixture was stirred at 70°C for 12hrs.

FT-IR (KBr, cm^{-1}): 3432.78 (O-H str), 2956.04 (asym -CH_3 str), 2917.58 (asym -CH_2 str), 2879.12 (sym -CH_3 str), 1451.57 (C-O str), 1100-1015 (C-O-C str), 749.75 (C-Cl str)

^{1}HNMR (500 MHz, $CDCl_3$): δ 0.85 (t, 3H, -C$\underline{H}_3$), δ 1.37(q, 2H, -C$\underline{H}_2$-), δ 3.39 (s, 6H, -C$\underline{H}_2$-O-), δ 3.59 (m, 6H, -C$\underline{H}_2$-Cl), δ 3.72 (m, 6H, -CH-C$\underline{H}_2$-O-), δ 3.98 (m, 3H, $\underline{H}$C-O-)

^{13}C NMR (125 MHz, $CDCl_3$): δ 7.55 (-$\underline{C}H_3$), δ 23.12 (-$\underline{C}H_2$-), δ 43.34 (-$\underline{C}$-CH_2-CH_3), δ 45.75 (-$\underline{C}H_2$-Cl), δ 70.00 (-$\underline{C}$H-OH), δ 72.12 (-$\underline{C}H_2$-O-), δ 78.98 (-$\underline{C}$-CH_2Cl)

2.4. Synthesis of azide terminated hyperbranched polyether polyol (HBP-N_3)

The above synthesized chlorinated hyperbranched polyol (5 gm, 1 eq) was dissolved in a solvent mixture of acetonitrile and water (8:1). To this, excess Sodium azide (7.2gm, 7.5 eq) was added portion wise. The resulting reaction mixture was stirred for 36 hrs at 75°C. After completion of the reaction, the solvent was evaporated. The product was extracted in chloroform and washed with brine solution for 2 times. The organic layer was collected and dried over sodium sulfate. The product HBP-N_3 was obtained after evaporating the solvent.

FT-IR (KBr, cm^{-1}): 3432.78 (O-H str), 2956.04 (asym -CH3 str), 2917.58 (asym -CH_2 str), 2879.12 (sym -CH_3 str), 2102.53 (N_3 str), 1451.57 (C-O str), 1100-1015 (C-O-C str)

^{1}HNMR (500 MHz, $CDCl_3$): δ 0.82 (t, 3H, -C<u>H</u>$_3$), δ 1.31(q, 2H, -C<u>H</u>$_2$-), δ 3.34 (m, 6H, -C<u>H</u>$_2$-N_3), δ 3.45 (m, 6H, -C-C<u>H</u>$_2$-O-), δ 3.5-3.7 (m, 6H, -CH-C<u>H</u>-O-), δ 3.92 (m, 3H, <u>H</u>C-OH)

^{13}C NMR (125 MHz, $CDCl_3$): δ 7.39 (-<u>C</u>H_3), δ 23.12 (-<u>C</u>H_2-), δ 42.93(-<u>C</u>-CH_2-CH_3), δ 53.27 (-<u>C</u>H_2-N_3), δ 65.52 (-<u>C</u>H_2-O-), δ 72.61 (-<u>C</u>H-OH), 78.86 (-CH_2O-<u>C</u>-CH_2-N_3)

2.5. Synthesis of alkyne terminated MWCNT (CNT-Alkyne)

1.0g of pristine CNT was treated with 23ml of 50 wt% nitric acid in a round bottom flask. The mixture was refluxed for 50 hours. The resulting solution was diluted with a large amount of de-ionized water and filtered. The filtrate was washed several times with de-ionised water until it reached a pH of 7, which was further dried at 120°C for 24h. Finally, 0.91 g of carboxyl functionalised CNT (CNT-COOH) was obtained. To the resulting CNT-COOH (0.2g), excess thionyl chloride (4ml) was added in a round bottom flask and then stirred for 24 hours at 70°C respectively. After this, excess $SOCl_2$ was removed under reduced pressure. Then the flask was cooled by an ice bath. To the reaction mixture, a mixed solution of propargyl alcohol (2 ml, 33.8 mmol), chloroform (4 ml) and anhydrous triethyl amine (2 ml, 14.34 mmol) were added drop wise over a period of 0.5h under stirring. The resulting mixture was stirred at 0°C for one hour followed by stirring at room temperature for 24 hrs. The product was filtered under vacuum, the filter cake was washed with THF and distilled water several times. The obtained CNT-Alkyne was dried under vacuum at 60°C for 24 hrs. The as prepared CNT-COOH and CNT-Alkyne were characterized by using FT-IR, TGA and FE-SEM techniques.

2.6. Procedure for Click reaction between of HBP-N_3 and CNT-Alkyne (CNT-HBP)

150 mg of CNT-Alkyne was dispersed in 30 g of DMF in a round bottom flask. The mixture was sonicated for 10 minutes and then flushed with nitrogen. Then 27 mg of CuI, 100mg HBP-N_3 and 0.02g of DIPEA were added to the above solution. The reaction mixture was stirred under nitrogen atmosphere at 70°C for 12 hours. The reaction mixture was terminated by cooling the reaction flask in ice bath followed by exposure to air. The reaction mixture was diluted with 10

ml DMF followed by ultrasonication for 10 minutes. The resulting mixture was filtered and washed with THF, aqueous ammonium hydroxide solution and pure water thrice. The resulting product was dried under vacuum to obtain CNT-HBP (Figure 1).

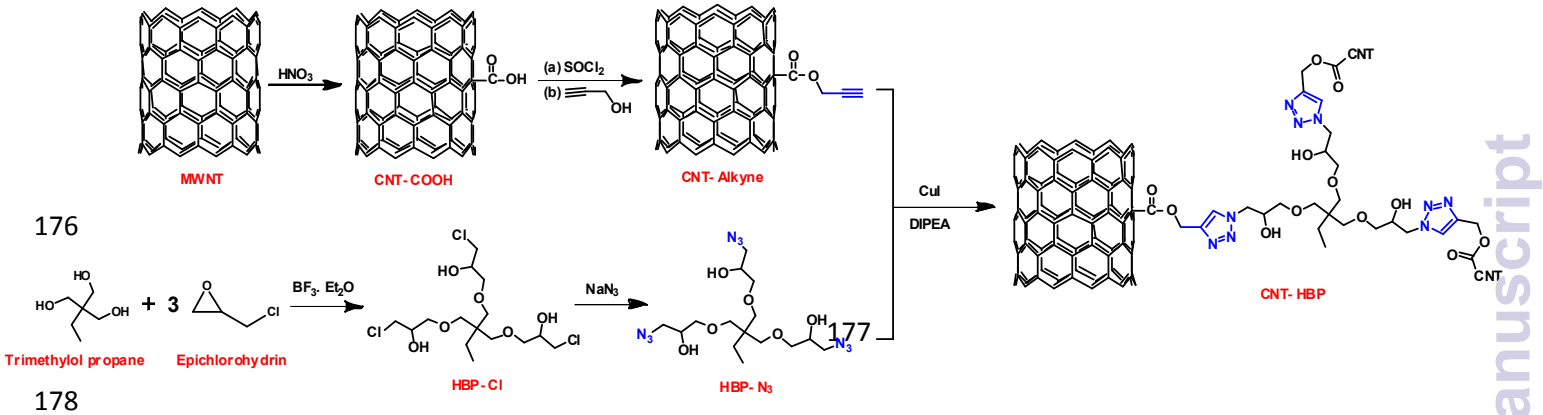

Fig. 1 Synthetic protocol for hyperbranched polyol Functionalized MWCNT (CNT-HBP) through azide-alkyne click chemistry

2.7. Synthesis of Polyurethane- CNT hybrid composites (CNT-PU)

Calculated amount of CNT-HBP (0.1%, 0.2%, 0.5%, 1% and 2% with respect to total weight) and H_{12}-MDI (0.98 g, 3.73 mmol) were taken in a round bottom flask. To this 2.5g of cellosolve acetate was added as a solvent. The mixture was sonicated for half an hour and stirred at 60°C for three hours. To this solution a mixture of PTMG (1g, 1 mmol) and TMP (0.15g, 1.1 mmoles, 15 weight % with respect to PTMG) dissolved in cellosolve acetate was added drop wise slowly. In all the hybrid composites, OH and NCO ratio was maintained as 1:1.2. The mixture was stirred at 65°C for 8 hours under inert atmosphere. Different CNT-PU hybrid composite films were casted on a tin foil supported over a glass plate by a manual driven square applicator, with adding one drop of 5% DBTDL in MIBK as catalyst and one drop Tagostab as surfactant. The excess NCO present in the hybrid films were moisture cured at 30°C and laboratory humidity condition (25–30%) for 15 days. The supported films were extracted after amalgamation and cleaning (Figure 2).

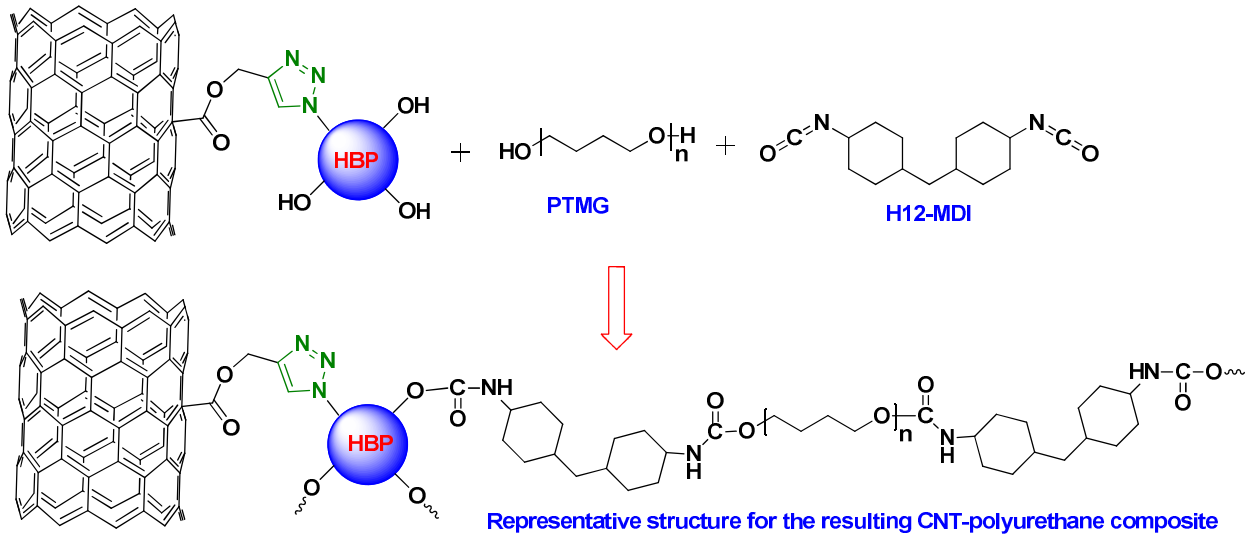

Fig.2 Synthesis of polyurethane-CNT hybrid composites

3. Results and discussion

3.1. Hyperbranched polyether polyol functionalised carbon nanotube

The development of compatible hyperbranched polymer is very essential for the functionalization of CNTs. This entails high precision at various stages involved in the synthesis of the final hyperbranched polymer. For this reason, firstly a chlorinated hyperbranched polyether polyol (HBP-Cl) was prepared and which was converted into HBP-N_3. The formation of HBP-Cl from Trimethylolpropane and epichlorohydrin is evident from the disappearance of epoxide stretching frequencies around 3050 and 900 cm^{-1} and the formation of ether stretching at 1100-1000 cm^{-1} in FT-IR; The appearance of new peaks related to ether linkage at δ 3.75, δ 3.98 in ^{1}H-NMR and δ72.21, δ 70.13 in ^{13}C-NMR; the presence of (M+Na) m/z peak at 435 in ESI-MS spectra and also the absence of peaks related to epoxide at δ 2.6, δ 2.8, δ 3.2 in ^{1}H-NMR and peaks at δ 51.35, δ 46.89 in ^{13}C-NMR simultaneously, is a substantial confirmation of the as prepared HBP-Cl. Further the nucleophilic substitution of HBP-Cl with azide groups for the formation of HBP-N_3 was corroborated with the disappearance of C-Cl stretching at 750 cm^{-1} and the appearance of sharp and intense peak at 2100 cm^{-1} in FT-IR studies; the disappearance of peaks at δ 3.59 (-C$\underline{H}_2$-Cl) in ^{1}H-NMR and δ 45.75 (-$\underline{C}H_2$-Cl) in ^{13}C-NMR; simultaneously the formation of peaks at δ 3.34 (-C$\underline{H}_2$-N_3) in ^{1}H-NMR and δ 53.27 (-$\underline{C}H_2$-N_3) in ^{13}C-NMR; the presence of (M+Na) m/z peak at 454 in ESI-MS spectra. (For ^{1}H-NMR, ^{13}C-NMR, FT-IR and

ESI-MS spectra refer Supplementary information) Once HBP-N_3 was synthesized the immediate step involved is the modification of CNT surface. Since pristine CNTs cannot be used for the attachment of HBP-N_3, it is obligatory that CNT undergoes certain changes. Thus CNTs were initially oxidized to form CNT-COOH, then to CNT-Alkyne by treatment with propargyl alcohol. The click reaction between the azide terminated HBP-N_3 and CNT-Alkyne, confirmed by the disappearance of azide and alkyne stretching peaks around 2100-2200 cm^{-1} in the FTIR spectra. Thermo gravimetric analyses were also performed in order to determine the changes in thermal stability of various samples. The overlay image of various TGA graphs is shown in Figure 3(a). For instance, the onset decomposition temperatures of pristine CNT, CNT-COOH, CNT-Alkyne and CNT-HBP are 583.90°C, 572.14°C, 470.72°C, 379.94°C respectively. The thermal stability of the CNT decreases with subsequent surface modification (Table S 1).

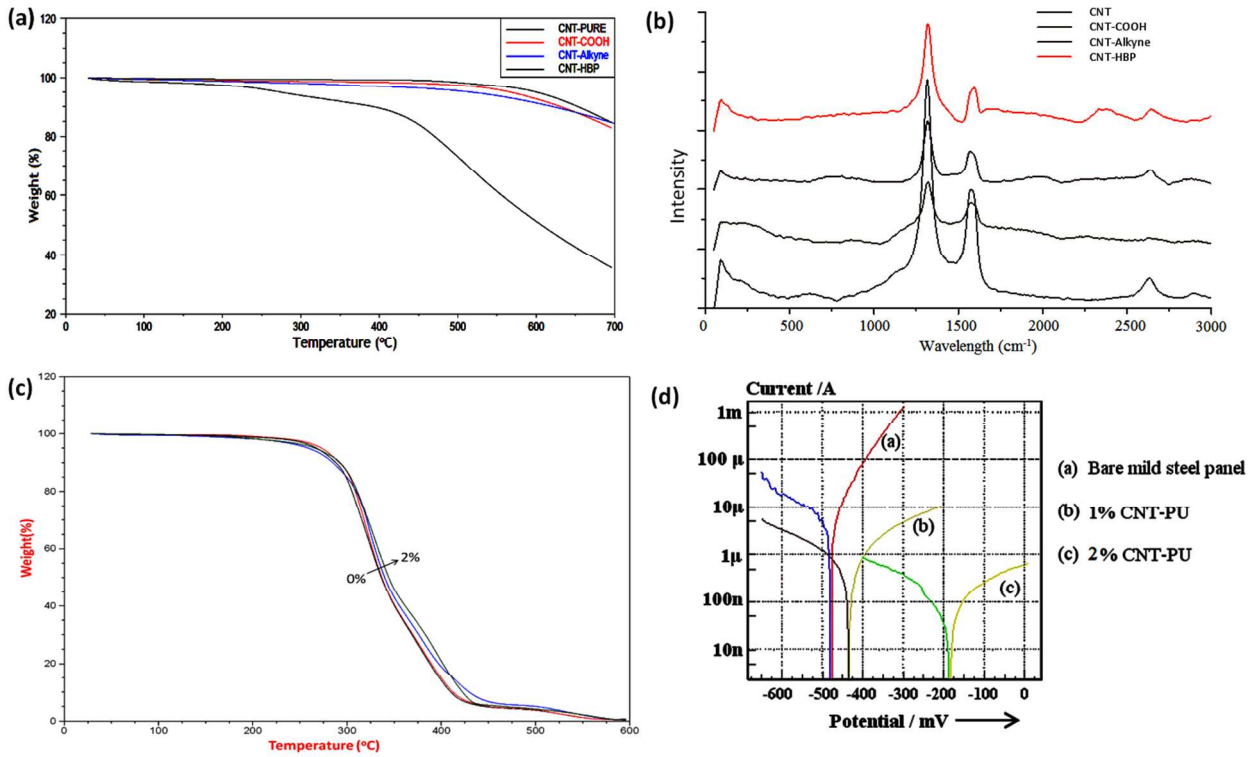

Fig. 3 (a) TGA thermograms (b)Raman Spectra of pristine CNT, CNT-COOH, CNT-Alkyne and CNT-HBP; (c) TGA thermograms of 0%,0.5%, 1% and 2% CNT-PUs (d) The polarization curves of different CNT-PU coatings along with the bare metal valuated by the Tafel method in a 5% NaCl solution.

X-ray Diffraction peaks of the CNT samples reveal two prominent peaks at 26.5° and 42° (Figure S 10) which can be attributed to the (002) and (100) plane of hexagonal graphite.[31] However

there is a distinct change in the intensities of modified CNTs as compared to the pristine CNT. In the pristine CNT the van der waals force of attraction holds the nanotube bundles together. Following the acid treatment, it is evidently seen in TEM and FE-SEM images that nanotubes become loosely bundled (Figure 4 and Figure S 11). This is credited to the decrease in the van der walls force of attraction between nanotubes which leads to a reduced inter-tubular interaction as compared to pristine CNT.[32] Since the aim of the work is to obtain CNTs that are soluble for use as composite materials, it is necessary to have substantial interaction between nanotube and also its immediate surroundings. Thus in the present study CNT surface is anchored with a hyperbranched polyol, so as to ensure the solubility of CNTs and also facilitate the interaction between tubes through hydrogen bonding between the hyperbranched polyols. The soft segments of HBP impart inherent amorphous nature to the CNT, which is observed as a decrease in intensity of the XRD peak.

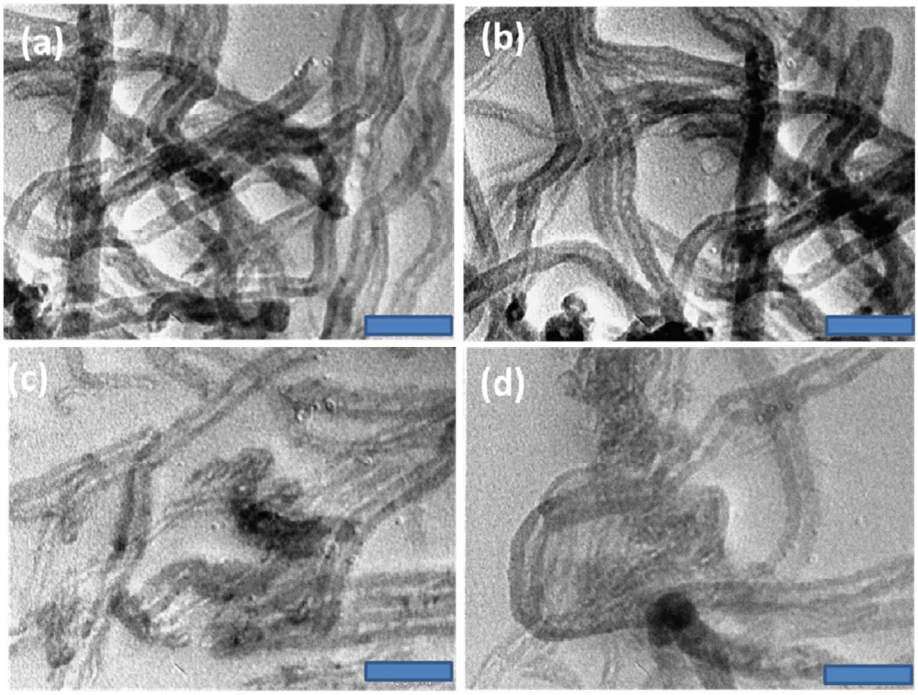

Fig. 4 TEM images of (a) pristine CNT, (b) CNT-COOH, (c) CNT-Alkyne, (d) CNT-HBP (scale bar indicates 50 nm)

Raman analysis also clearly reveals the difference in each of the modified CNTs. The peak at 1312.42 cm^{-1}corresponds to CNT and 1318.91cm^{-1} for other functionalized CNT (Table S 2) corresponds to D-band ('D' for defect or disorder). From the experimental observations it is

evident that there is a significant shift in D-band with modification of CNT surface. This is an outcome of the disorders present and symmetry lowering. The appearance of D-band in carbonaceous materials is because of one-phonon second order Raman scattering process, which involves both elastic and inelastic scattering.[33,34] Jorio *et al*.[35] reported that the D-band shows a strong dependence on the excitation wavelength. The polarization dependence studies carried out, suggest that origin of D-band is because of disorder and finite size effect of carbons. There is also evident change in the I_D/I_G ratios in each modified CNT. I_D/I_G ratio provides information on the alignment of CNT. G-band (G stands for graphite) originates from first order Raman effect. G-band which comprises of six modes (according to group theoretical analysis) for each symmetrical mode in the nanotubes, the vibration of atoms are either along the tube axis (G+) or along the circumferential direction(G-). There is also a definite change in the intensities of G-band from the Figure 3(b). The G-band in CNT corresponds to optical phonon mode between the two dissimilar carbon atoms in the unit cell. It is known to originate from the sp^2 carbons present in the CNT.[36]

In the present study the CNT surface is anchored with hyperbranched polyol, so as to ensure the solubility of CNTs and also facilitate the interaction between tubes through hydrogen bonding between the hyperbranched polyols. It is observed that the surface modified CNTs such as CNT-COOH, CNT-Alkyne and CNT-HBP show improved dispersion stability in various solvents. Moreover, CNT-HBP shows higher solubility behaviour because of its surface hydroxyl functional groups. The presence of carboxyl, alkynyl and hydroxyl groups facilitate swift dispersion of CNT-COOH, CNT-Alkyne and CNT-HBP in polar solvents because of their inherent polar nature. This behaviour may be due to formation of hydrogen bonds with solvent systems. The poor dispersion stability of the modified CNTs in toluene solvent is accounted to the non-polar nature of the solvent system. (Figure S 12 and Table S 3)

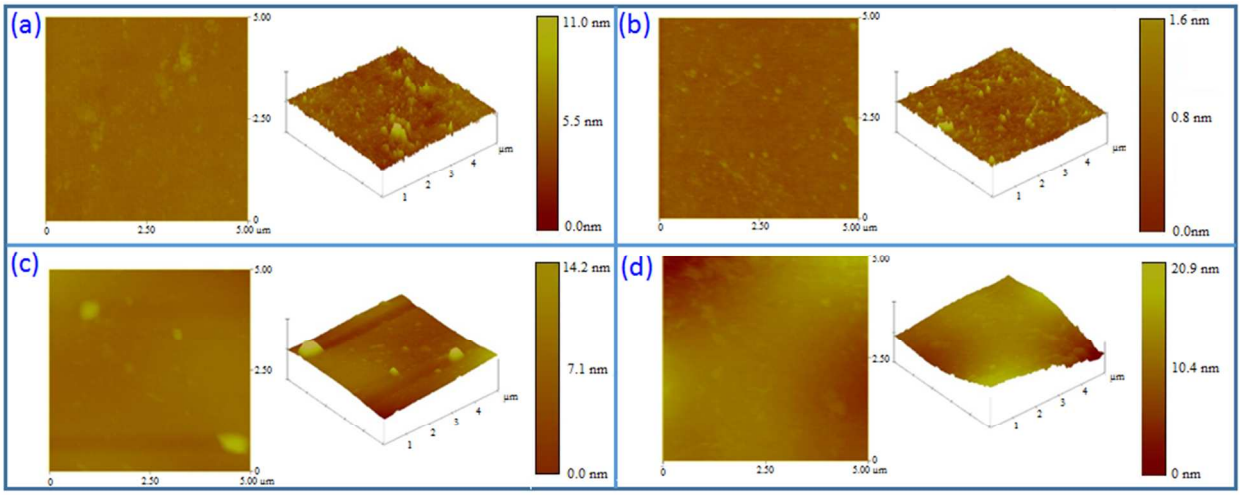

Fig. 5 AFM images of (a) 0%CNT-PU (b) 0.5%CNT-PU, (c) 1% CNT-PU (d) 2% CNT-PU

3.2. Functional CNT-HBP Polyurethane-urea hybrid composites (CNT-PUs)

Once the properties of CNT-HBP were established, the next step is to covalently link it to the polyurethane matrix so as to fabricate functional hybrid composites. The successful synthesis of carbon nanotube incorporated-polyurethane hybrids is based on the complete absence of free –NCO peak around 2270 cm^{-1} in the FT-IR spectra (Figure S 5), which indicates complete moisture curing of the polyurethanes. The observed absorption bands (cm^{-1}) at 3050–3700 (–NH stretch), 2800–3000 (–CH stretch consisting of asymmetric –CH3 stretch at 2957, asymmetric –CH_2 stretch at 2920, symmetric –CH_3 stretch at 2872 and symmetric –CH_2 stretch at 2851 cm-1), 1600–1800 (-C=O stretching of amide I), 1500–1600 (amide II stretch consisting of a mixture of peaks δ_{N-H}, υ_{C-N} and υ_{C-C}),1394 (δ_{CH2}symm/assym), 1215–1350 cm^{-1} (amide III, υ_{C-N}), 766 (amide IV due to –NH out of plane vibration) and 720 (–CH_2 rocking) supports the formation of polyurethanes. Neat polyurethane (0% CNT-PU) has a highly smooth surface, whereas the incorporation of CNT transforms the PU film into a rough and fractured micro structure with many pleats (Figure S 11). The effect of incorporating CNTs in the organization of PU matrix could be correlated with the increase in the density of pleats with the percentage of CNT, which could be verified by the surface roughness analysis from AFM (Figure 5). The formation of these rough surfaces facilitates high elongation at break and tensile strength of the polyurethane film.[37]

Table 1 Mechanical properties of CNT-PU hybrids (from UTM analysis)

Sample code	Tensile strength (N/mm^2)	Elongation at break(%)
0%CNT-PU	1.25	10.74
0.5%CNT-PU	2.031	40.5
1%CNT-PU	4.31	136.5
2%CNT-PU	6.25	146.3

XRD analysis also confirm the increase in the crystallinity of CNT-PUs with the CNT-HBP loading (Figure S 10). From UTM analysis (Figure S 13 and Table 1), it is observed that both tensile strength and elongation at break increases with CNT loading. Since, CNTs are thermo-oxidative stable materials[38]; their incorporation enhances the thermal conductivity of polyurethane hybrid composites and therefore increases its thermal stability (Figure 3(c) and Table 2). The reason for improvement of thermal and mechanical stability of these hybrid films are due to the formation of urethane linkages by the hydroxyl groups present on the surface of CNT-HBP. The formed urethane linkages are capable of cross-linking through hydrogen bondings with the polyurethane matrix, which also imparts hydrophobicity to the hybrids which is realized from water contact angle measurements (Figure S 14).Electrochemical polarization curves (Figure 3(d) and Table 3) from the Tafel plot suggests an improvement in the polarization resistance and deterioration in the corrosion rate amongst different CNT-PU films. This might be due to the formation of more cross-linked structures with increasing the CNT-HBP content, which restricts the penetration of corrosive species by acting as a strong physical barrier.

Table 2 TGA profile of various CNT-PUs

Sample code	Onset decomposition Temperature (T_{ON}) (^oC)	10%, wt loss temperature (T_{d10}) (^oC)	50%, wt loss temperature (T_{d50}) (^oC)	% wt remaining at 350^oC
0%CNT-PU	247.02	286.67	335.45	40.08
0.5%CNT-PU	251.91	284.40	336.02	40.09
1%CNT-PU	254.45	291.21	339.42	42.61
2%CNT-PU	256.34	292.34	343.39	45.90

Table 3 The electrochemical parameters measured from the Tafel plots of different CNT-PU hybrid coatings along with bare metal.

Sample code	*Coating thickness (μm)*	*Ecorr (mV)*	*I_{corr} (nA/cm2)*	*Polarization resistance (Rp) (kOhm cm^2)*	*Corrosion rate (C_R) (mm/yr)*
Bare mild steel panel	-	-476.6	3.86×10^3	8.85	0.047
1%CNT-PU	67	-474.4	1.12×10^3	490.64	0.012
2%CNT-PU	69	-200.0	164	3502.07	0.0019

Thus the cross-linking density of CNT-PU increases with increase in the CNT percentile. Thus, CNT-PU films are an excellent barrier to atmospheric moisture and oxygen. Such high cross-linking of CNT-HBP with polyurethanes instills shape recovery property to CNT-PU hybrid materials, which were examined by using UTM instrument in tensile mode. It is observed that, with increase of CNT loading, the shape recovery nature of the polyurethane film increases. First the samples were elongated up to their break point at room temperature using UTM. The elongated samples were removed from UTM and kept at 60°C for recovery. The sample recovered its original shape within 10 sec of heat treatment and the process was repeatable (Figure 4 and Table 4). The shape recovery property of CNT-PU hybrids was attributed to the excellent mechanical stability of the CNT and high thermal conductivity coefficient. The shape recovery of CNT-PUs depends on the presence and volume fraction of the CNT-HBP in the polyurethane film. Experimental studies reveal that the addition of CNT-HBP to PU lowers the unrestrained recoverable strain limit and increases the attainable controlled recovery stress . The particles are forced to store internal elastic strain energy during elongation. This mechanism restricts the generation of large recoverable strain, imparts higher recoverable force levels. The stored elastic strain energy in the particles is released once the film is unloaded. The temperature provided during the process help in rapid shape recovery. The transaction between recoverable displacement and force is an important characteristic of the shape memory CNT-PUs. The film with 2% loading was found to be optimum which showed a 100% shape recovery. CNT-PUs were also treated with different bacterial and fungal stains in order to estimate its tolerance to microbial attack. It is observed that the films with higher CNT-HBP content showed superior anti-microbial properties (Figure S 15).

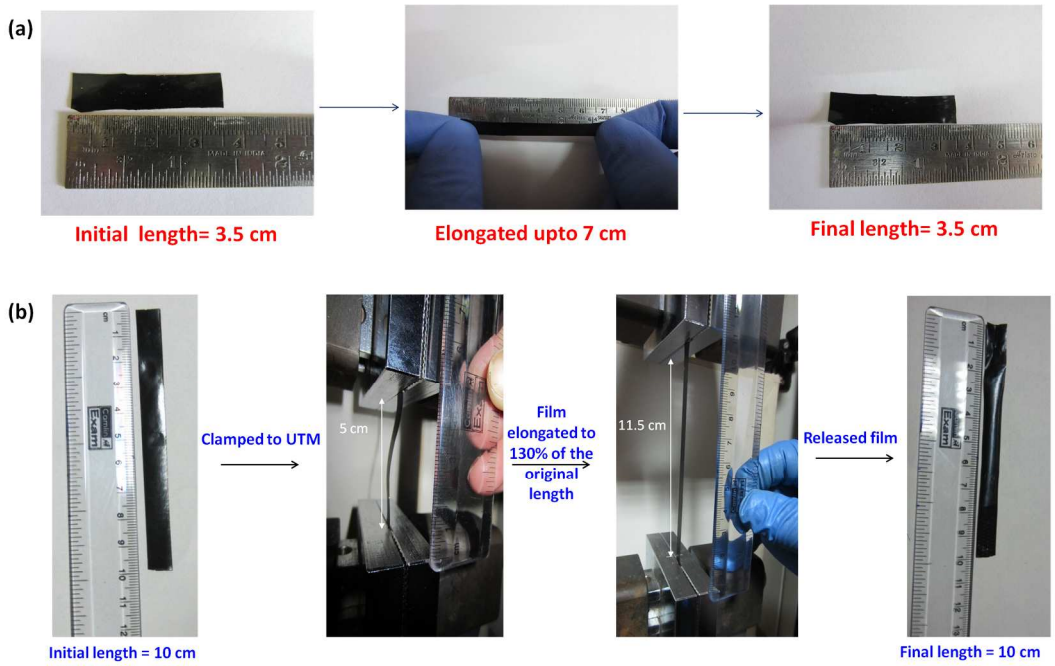

Figure 4 Shape recovery tests of 2% PUCNT film (a) manual and (b) UTM

Table 4 Shape recovery behavior of various CNT-PU samples

Sample code	% Elongation	100 % Shape recovery time (approximately)	
		Room Temp.	At 60°C
0.5% CNT-PU	30	40 sec	20 sec
1% CNT-PU	130	25 sec	10 sec
2% CNT-PU	130	20 sec	10 sec

4. Conclusions

The past decade has shown a remarkable improvement in the carbon nanotechnology. However little has been researched about polyurethane based hybrids. We have successfully synthesized multifunctional Polyurethane-urea-CNT hybrid composites with superior mechanical, thermal, hydrophobic, antimicrobial and anticorrosive properties along with excellent shape recovery behavior. These properties are mainly due to uniform distribution of decorated CNTs in polyurethane-urea-CNT hybrid composite matrix as well as improved cross-linking. This improvement is due to the presence of extra hydroxy groups on decorated CNTs as compared to

neat polyurethane. Though the research is fundamental, it can be exploited for applications as smart coatings for different substrates such as metals, textiles, leather, fiber etc. The shape recovery with stimuli-responsive nature along with hydrophobicity can be exploited for smart wrinkle resistant textiles whereas the moisture curing, corrosion resistance, antimicrobial properties and hydrophobicity can be exploited for smart high performance coatings on metals in moist marine environments. Thus Polyurethane-urea-CNT hybrid composites could represent a new exciting direction that may open up opportunities in various scientific fields.

Acknowledgements

The present research was supported by CSIR under the Intel-Coat Project (CSC-0114). The authors would like to extend their thanks to the Director, CSIR- IICT for permitting the work to be carried out.

Supporting Information

Tables related to TGA, Raman, solubility. Figures related to FT-IR, 1H-NMR, 13C-NMR, ESI-MS, XRD, FE-SEM, solubility test, UTM, Contact angle, antimicrobial result.

REFERENCES

1. S.Iijima, *Nature*, 1991, **354**, 56–58.
2. J.P.Salvetat, J.M.Bonard, N.H.Thomson, N. H., A.J.Kulik, L.Forro, W.Benoit and L.Zuppiroli, *Appl. Phys. A: Mater. Sci. Process*, 1999, **69**, 255-260.
3. X.Wan and J.Dong, *Phys. Rev. B: Condens. Matter*, 1998, **58**, 6756– 6759.
4. (a) D.Tasis, N.Tagmatarchis, A.Bianco and M.Prato, *Chemical Reviews*, 2006, **106**, 1105-1136. (b) T.Fukumaru, T.Fujigaya and N.Nakashima, *Macromolecules*, 2013, **46**, 4034-4040
5. M.Ouyang, J.L.Huang and C.M.Lieber, *Accounts of chemical research*, 2002, **35**, 1018-1025.
6. D.Qian, E.C.Dickey, R.Andrews and T.Rantell, *Appl. Phys. Lett.*, 2000, **76***,* 2868-2870.
7. M.J.Biercuk, M.C.Llaguno, M.Radosavljevic, J.K.Hyun, A.T.Johnson and J.E.Fischer, *Appl. Phys. Lett.*, 2002**, 80***,* 2767-2769.
8. M.Cadek, J.N.Coleman, V.Barron, K.Hedicke and W.J.Blau, *Appl. Phys. Lett.*, 2002, **81***,* 5123-5125.
9. (a) C.Velasco-Santos, A.L.Martinez-Hernandez, F.T.Fisher, R.Ruoff and V.M.Castano, *Chem. Mater.* 2003, **15***,* 4470-4475. (b) L.C.Tang, Y.J.Wan, K.Peng, Y.B.Pei, L.B.Wu, L.M.Chen and G.Q.Lai, *Composites Part A: Applied Science and Manufacturing*, 2013, **45**, 95 (c) L.C.Tang, H.Zhang, J.H.Han, X.P.Wu and Z.Zhang, *Composites Science and Technology*, 2011, **72**, 7-13.
10. A.Lendlein and R.Langer, *Science*, 2002,**296**, 1673-1676.
11. B.S.Lee, B.C.Chun, Y.C.Chung, K.I.Sul and J.W.Cho, *Macromolecules*, 2001, **34**, 6431-6437.
12. M.Wang, X.Luo and D.Ma, *European polymer journal*, 1998,**34**, 1-5.
13. L.S.Schadler, S.C.Giannaris and P.M.Ajayan, *Appl. Phys. Lett.* 1998,*73*, 3842-3844.
14. P.Liu, *Eur. Polym. J.*, 2005, **41**, 2693–2703.
15. J.N.Coleman, A.B.Dalton, S.Curran, A.Rubio, A.P.Davey and A.Drury, *Adv. Mater.*, 2000, **12**, 213-216.
16. P.Singh, S.Campidelli, S.Giordani, D.Bonifazi, A.Bianco and M.Prato, *Chem. Soc. Rev.*, 2009, **38***,* 2214-2230.

17. J.Feng, J.Sui,W.Cai and Z.Gao, *Journal of composite materials*, 2008, **42**, 1587-1595.

18. V.C.Moore, M.S.Strano, E.H.Haroz, R.H.Hauge, R.E.Smalley, J.Schmidt and Y.Talmon, *Nano Letters*, 2003, **3**, 1379-1382.

19. O.Matarredona, H.Rhoads, Z.Li, J.H.Harwell, L.Balzano and D.E.Resasco, *The Journal of Physical Chemistry B*, 2003, **107**, 13357-13367.

20. M.J.O'Connell, P.Boul, L.M.Ericson, C.Huffman, Y.Wang, E.Haroz and R.E.Smalley, *Chemical Physics Letters*, 2001, **342**, 265-271.

21. C.A.Dyke and J.M.Tour, *The Journal of Physical Chemistry A*, 2004, **108**, 11151-11159.

22. S.Bose, R.A.Khare and P.Moldenaers, *Polymer*, 2010, **51**, 975-993.

23. R.G.Mendes, A.Bachmatiuk, B.Büchner, G.Cuniberti and M.H.Rümmeli, *Journal of Materials Chemistry B*, 2013, **1**, 401-428.

24. M.Kumar and Y.Ando, *Journal of nanoscience and nanotechnology*, 2010, **10**, 3739-3758.

25. J.T.Sun, C.Y.Hong and C.Y.Pan, *Polymer Chemistry*, 2011, **2**, 998-1007.

26. A.M.Caminade and J.P.Majoral, *Chemical Society Reviews*, 2010, **39**, 2034-2047.

27. V.V.Rostovtsev, L.G.Green, V.V.Fokin and K.B.Sharpless, *Angewandte Chemie*, 2002,**114**, 2708-2711.

28. W.H.Binder and R.Sachsenhofer, *Macromolecular Rapid Communications*, 2007, **28**, 15-54.

29. S.Campidelli, B.Ballesteros, A.Filoramo, D.D.Díaz, G.De la Torre, T.Torres and J.P.Bourgoin, *Journal of the American Chemical Society*, 2008, **130**, 11503-11509.

30. Herbert P. Price, *US pat.* US3033803, 1962.

31. W.Li, C.Liang, W.Zhou, J.Qiu, Z.Zhou, G.Sun and Q.Xin, *The Journal of Physical Chemistry B*, 2003,**107**, 6292-6299.

32. Q.Shi, D.Yang, Y.Su, J.Li, Z.Jiang, Y.Jiang and W.Yuan, *Journal of Nanoparticle Research* 2007, **9**, 1205-1210.

33. R.Saito, A.Jorio, A.G.S.Filho, G.Dresselhaus, M.S.Dresselhaus and M.A.Pimenta, *Physical review letters,* 2002, **88**, 027401-027401.

34. S.Osswald, M.Havel and Y.Gogotsi, *Journal of Raman Spectroscopy*, 2007, **38**, 728-736.

35. A.Jorio, G.Dresselhaus, M.S.Dresselhaus, M.Souza, M.S.Dantas, M.A.Pimenta and H.M.Cheng, *Physical review letters*, 2000, **85**, 2617-2620.

36. H.M.Heise, R.Kuckuk, A.K.Ojha, A.Srivastava, V.Srivastava and B.P.Asthana, *Journal of Raman Spectroscopy*, 2009, **40**, 344-353.

37. J.Huang, H.Zhang and Q.Zhang, *Journal of Wuhan University of Technology-Mater. Sci. Ed.*, 2012, **27**, 608-614.

38. H.Xia and M.Song, *Soft Matter*, 2005, **1**, 386-394.